Personalized Osteotomies to Correct Flatfoot

Andrew S. Cheng[1]

[1]Northwest High School, Germantown, MD, USA
[1]andrew.cheng.taotao@gmail.com

Abstract— Flatfoot deformity can cause pain, increase the risk of arthritis, limit mobility, and make the body susceptible to injuries. Traditional osteotomy procedures, which involve surgically reconstructing the bones, can be enhanced with modern technologies. This paper explores the use of artificial intelligence (AI) and 3D modeling to personalize and improve the precision of flatfoot surgeries. We focus on two key goals: using AI to design custom osseous wedges for correcting the deformity and quantitatively measuring plantar pressure during surgery to adjust the foot to normal bony structure, maximizing the chance of restoring the foot to its normal function. Our approach introduces a novel pipeline that uses AI-based segmentation of CT images to create detailed 3D models of a patient's foot bones, enabling simulation of surgical corrections tailored to individual anatomy. We also propose an intra-procedural synthetic AI model to assist with real-time adjustments during surgery, dynamically guiding alignment and corrections based on the patient's unique anatomy. Additionally, we aim to collect a large dataset of plantar pressure measurements from normal feet under surgical conditions to establish benchmark metrics for plantar pressure. Achieving a post-surgical pressure distribution that matches a healthy foot's metrics indicates a successful outcome. The proposed personalized, AI and data driven method might enhance the accuracy, efficiency, and overall surgical outcomes of flatfoot osteotomies.

Keywords— "AI, flatfoot, osteotomy, 3D, simulation, benchmark metrics, plantar pressure"

I. INTRODUCTION

A flatfoot deformity occurs when the medial longitudinal arch of the foot collapses that can lead to pain and moving restriction. This condition may result in long-term issues such as arthritis and tendinopathy that affect children and adults. When conservative treatments fail, surgeons may resort to complex procedures like osteotomies to realign the bones and improve foot function. However, it is challenging to achieve the proper structural corrections with those surgical procedure since the variability of foot anatomy make it hard to restore to normal foot structure.

This paper addresses two key challenges in flatfoot osteotomies:

- Can artificial intelligence (AI) aid in designing the restored bony structures of the foot before surgery?
- Can the stress concentration and load distribution on the plantar surface be quantitatively measured during surgery to ensure the bony corrections restore normal foot function before soft tissues are closed?

Surgeons often rely on a trial-and-error approach to determine the optimal size of bone graft wedges, particularly for procedures like Evans and Cotton osteotomies, which introduce the difficulty of accurately predicting the correction required to achieve optimal foot alignment. Studies have shown that the lack of standardized guidelines or predictive tools results in variability in graft sizing, which may affect both these procedures' short-term and long-term outcomes [1, 2]. Those methods can prolong the procedure and lead to unnecessary bone graft waste. For example, in the Evans osteotomy, which involves lateral column lengthening, the exact wedge size necessary to restore the proper relationship between the forefoot and hindfoot is often determined intraoperatively, based on visual and tactile assessment. Tennant et al. [1] illustrate a surgical guide to improve the accuracy of calcaneal osteotomies (including the Evans procedure) and suggest that the conventional method has limitations in achieving precise correction, hinting at a trial-and-error approach to find the right wedge size. Remoeo et al. [2] introduced a method to adjust the wedge size of Cutton osteotomies to achieve the desired correction for determining the optimal graft size. The proposed method could efficiently reduce the surgery time and trauma by pre-determining the size of grafts via an AI-driven approach.

Another challenge for the osteotomies for flat foot is to assess the functional restoration based on bony reconstruction. Orthopedists use a metal plate to see whether the footprints or the reconstructed feet resemble normal feet. However, this method cannot predict that the normal function of the foot can be restored after the surgery. Studies show that such intra-surgical measurement did not take dynamic factors into consideration, for example the plantar pressure under weight bearing [3]. An improved method is to replace the metal plate with force plate to measure the load distribution when the patient lying down because complete weight-bearing measurement is impractical during surgery. Thus, orthopedists heavily rely on post operative rehabilitation to ultimately restore foot functions, and then they can assess the functional outcomes. No precise predictions of the outcome can be made during surgery.

Recent advancements in AI and 3D simulation could open a new opportunity for the personalized flatfoot surgeries. AI driven flatfoot bone segmentation from CT images can build up the patient-specific 3D models, allowing surgeons to adapt to individual anatomy [4]. The work we propose solution that leverages AI to construct patient-specific bone grafts and employing quantitative methods to measure intraoperative plantar pressure distribution. This approach will ensure that the reconstructed foot can bear weight and distribute loads in a manner like a healthy foot. This paper explores the integration of AI-based 3D simulations and stress analysis for improving both structural and functional outcomes in flatfoot surgery. The end goal is to establish a new AI and data-driven approach to improve the general practice of flatfoot osteotomy.

II. METHODS

In this section, we focus on four critical components of this study. 1) We introduce the background of flatfoot biomechanics, symptoms, and existing surgical treatments, emphasizing the anatomical challenges imposed by flatfoot deformities and the limitations of current osteotomy procedures. We also briefly review a few related research works from surgical perspectives, such as Evans and Cotton's osteotomies. 2) We elaborate on the proposed method that involves the use of AI-Driven 3D modeling and simulation to build the foundation models of the flatfoot corrective surgeries. The AI integration with dynamic simulation enables surgeons to trial different osteotomy procedures virtually, optimizing correction angles and wedge sizes to each patient's unique anatomy. 3) We propose a quantitative evaluation of the reconstructed foot's function using an intra-procedure stress and pressure distribution measure. Surgeons can apply pressure distribution and weight-bearing measurement during the simulation for better surgical results. 4) We propose an intra-procedural synthetic AI model to assist in real-time flatfoot restoration feedback by dynamically adjusting to the patient's anatomy, guiding precise alignment, and optimizing correction angles throughout the procedure.

A. Background Review

Section 1: Biomechanics and Symptoms of Flatfoot

1. Normal Foot

We rely on our feet to move our bodies on the ground. A functioning foot should be flexible enough to keep our body balanced on different surfaces and absorb the shock when we jump or run. It also needs to be stiffened enough to propel our body forward during the push-off phase of each gait cycle. The arch of the foot plays an important role. It acts like a spring absorbing the impact of shock. It distributes the body weight across the sole and dynamically adjusts to different surfaces, maintaining the proper posture and alignment of the body and the stability and balance of the person. [5]
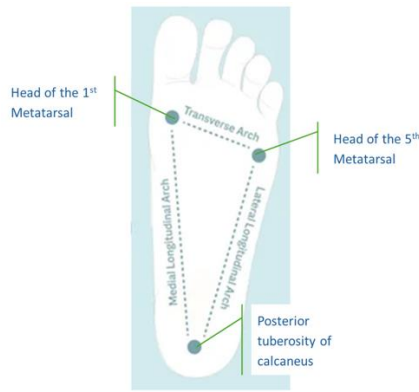
Figure 1. The three arches of foot

The foot has 3 arches: the medial, lateral and transverse arches (Figure 1).

(1) The medial longitudinal arch is the inner highest arch that running along the inner side of the foot from the heel to the forefoot. It is commonly referred to as "the arch" of the foot. Medial longitudinal arch provides shock absorption and helps distribute weight evenly across the foot. The medial arch stores mechanical energy during the stance of walking. The arch acts as a springboard to propel the foot forwarding during walking, running, enabling smoother movement.

(2) The lateral longitudinal arch is the flatter of the two longitudinal arches, which is located on the outer side of the foot, running parallel to the medial longitudinal arch. It provides stability and balance to the foot, especially when standing or during activities like walking on uneven surfaces. The lateral arch is lower and flatter, contributing more to support and load-bearing. The posterior tuberosity of the calcaneus takes most of the forces in a gait cycle.

(3) The transverse arch is represented as the width of the foot near the forefront foot (i.e., spanning from 1st to 5th metatarsals). It helps the body to maintain the balance while adapting to different surfaces during walking, running and stands. The transverse arch also helps evenly distribute body weight across the foot during standing and walking, reducing pressure on any single point.

The three arches of the foot form a steady triangle to support the body's weight. In a normal foot, the stress is concentrated at three primary points of contact: the heel (the tuberosity of calcaneus), the ball of the foot (the heads of the metatarsals), and the toes (phalanxes), particularly the big toe. These areas bear most of the body's weight when standing or moving. The three arches function differently to support our movements and balance our bodies. The medial longitudinal arch absorbs the shock when jumping or running; the lateral longitudinal arch stabilizes the foot and evenly spreads the load on longitude; the transverse arch distributes the load at latitude. The three arches coordinate to enable us to accomplish demanding athletic activities.

2. Flatfoot

Flatfoot is a condition characterized by the collapse or absence of the medial longitudinal arch of the foot. The navicular bone, located in the arch of the foot, may drop closer to the ground (Figure 2).
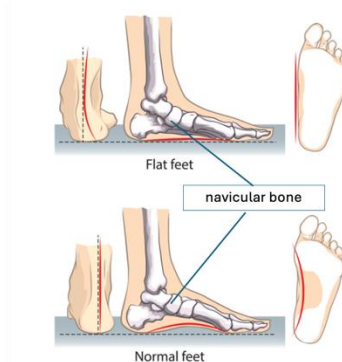

Figure 2: Flat vs. Normal foot rear, lateral, and bottom views

The talus, which forms ankle joints together with tibia and fibula, shifts medially and downward. This displacement pushes the talar head, causing increased pressure on the inside of the foot and contributing to the collapse of the arch. Consequently, the calcaneus, heel bone, angles outward to a valgus position when viewed from behind, rather than being aligned straight under the body; The front part of the foot may rotate outward, referred to as forefoot abduction. This misalignment can give the foot an "C-shaped" appearance when viewed from Figure 3.
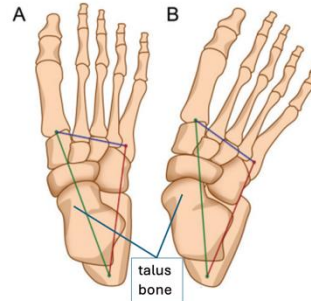

Figure 3: Normal vs Flat foot top view

In flatfoot, the weight-bearing shifts from the lateral side to the medial side of the foot, particularly to the medial side of the calcaneus, medial longitudinal arch, navicular bone, and the first metatarsal. It reduces the natural shock absorption provided by the arch of the foot. As the plantar fascia becomes overstretched in an attempt to compensate for the collapsing arch, increased stress concentration occurs in this region. The altered load distribution in the heel can cause strain in the calcaneal tendon, increase the risk of heel pain, and stress the posterior tibialis tendon (PTT) and deltoid ligament, leading to ankle instability because PTT and deltoid ligament are the primary stabilizers of the ankle joint. Eventually, the abnormal loading pattern of flat feet will result in foot fatigue, inflammation, and injuries.
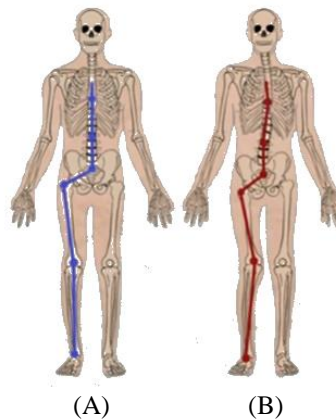

(A)   (B)
Figure 4: Alignment of upstream body
A. Normal foot aligned; B. Flatfoot misaligned

The changes in the load distribution in flatfoot alter the balance of the body and the kinetic chain of the upstream body, hence, the structure of upstream body (Figure 4). As the medial side of the foot bears the primary increase in stress, the body tries to balance the instability created by the collapsing arch by shifting some weight to the lateral side. This can overwork the peroneal tendons, which are located on the outside of the foot, potentially leading to peroneal tendonitis or lateral ankle sprains. Flatfoot can lead to overpronation which creates a correlated reaction that affects the alignment of the entire lower extremity. As the foot rolls inward, the tibia rotates inward as well, increasing torque on the knee joint. Inward rotation of the lower leg can create compensatory movements and altered posture in the hips and lumbar. The changes in stress on joints cause pain in knees, hip joint and lumbar spines, and increase the risk of developing conditions like knee osteoarthritis. The poor shock absorption, ankle instability and improper alignment of entire lower extremity make the body susceptible to injuries.

Section 2: Causes and Diagnosis of Flatfoot Deformity

Flatfoot deformity can manifest in both children and adults, with varying causes and degrees of severity. Pediatric flatfoot is often flexible and considered a normal part of growth, especially in toddlers, as physiologic ligamentous laxity tends to improve with age. However, for some children, the condition persists into adolescence or adulthood, particularly among those who are overweight or have genetic predispositions. Morley [6] documented flatfeet in 97% of 18-month-olds. Flatfeet were present in 54% of 3-year-olds and 26% of 6-year-olds. Body weight positively correlates to flatfeet. Flatfeet were present in 62% of obese, 51% of overweight, and 42% of young children with normal body weight. Children with flat foot by age 10 can hardly develop foot arches naturally. Children with a family history of flatfeet may be more likely to have persistent flatfeet as adults.

In adults, flatfoot can be acquired later in life due to posterior tibial tendon dysfunction and soft tissue failure, leading to a progressive flattening of the medial arch, hindfoot valgus, and forefoot abduction. The prevalence of flatfeet in adults is 15–23% [7]. Adult-acquired flatfoot deformity (AAFD), if left untreated, may lead to significant pain, gait abnormalities, and long-term disability [8]. An estimated 7%–15% of adults with developmental flatfoot eventually develop symptoms that lead them to seek medical attention [9].

Radiographic measurement is commonly used to evaluate osseous deformity of flatfoot. The measurements are used principally to evaluate longitudinal arch flattening, hindfoot valgus, and forefoot abduction is summarized in Table 1 [8] and visualized in Figure 5 and Figure 6 [8].

Radiographic Metrics of Foot Alignment			
		Alignment Angle (degrees)	
Metric	Construction	Normal	Flat Feet
Lateral view: assessment of longitudinal arch			
Talus-first Metatarsal angle (Meary angle)	Angle between the long axis of the talus and the long axis of the first metatarsal	0 (parallel)	Mild: >4 Moderate: >15 Severe: >30
Calcaneal inclination angle	Angle between the line at the plantar calcaneal surface and the horizontal plane	20 - 30	Pes planus: <18
Calcaneal-fifth metatarsal angle	Angle between the line at the plantar calcaneal surface and the line at the interior fifth metatarsal shaft	150 - 165	>170
Anteroposterior view: assessment of heel valgus and forefoot abduction			
Talocalcaneal angle (Kite angle)	Angle between the line bisecting the head and neck of the talus and the line parallel to the lateral surface of the calcaneus	>25 - 40	> 40 (heel valgus) < 25 (heal varus)
Talus-first metatarsal alignment	Line drawn along the long axis of the talus, extended into the forefoot, its orientation compared with that of the first metatarsal shaft	Talar axis angled slightly lateral to the shaft	Talar axis angled medial to the shaft
Talonavicular coverage angle	Angle between the articular surface of the talar head and the articular surface of the proximal navicular bone	0 (parallel)	>7

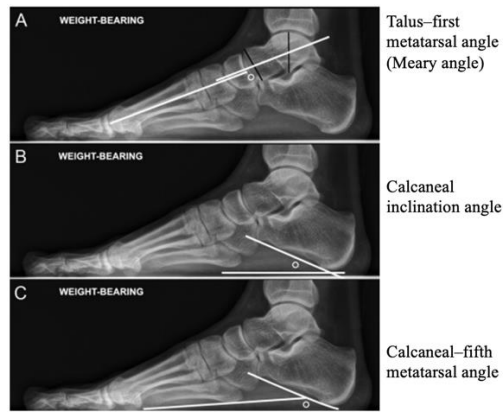Table 1 Commonly Used Radiographic Metrics of Foot Alignment

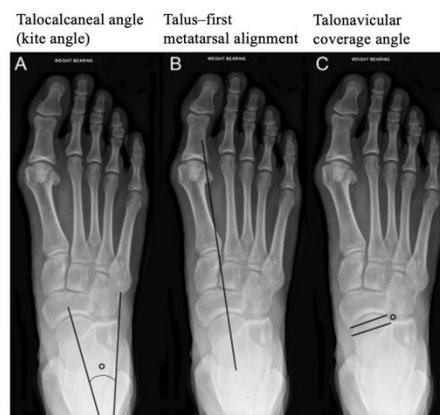Figure 5. Lateral view: assessment of longitudinal arch – Normal foot

Figure 6. Anteroposterior view: assessment of heel valgus and forefoot abduction – Normal foot

Flatfoot can manifest in two forms: a painless, flexible variant, which is a common part of growth and often asymptomatic, and a more severe, rigid type associated with underlying conditions like tarsal coalition or neurologic diseases. Diagnosis relies heavily on a thorough clinical history and physical examination to distinguish between normal flexible flatfoot and pathological rigid flatfoot. Alternative imaging modalities, such as X-rays or MR images could play an important role in assessment for diagnosis in more realistic cases.

Treatment for flexible, asymptomatic flatfoot is generally unnecessary, especially for pediatric flatfoot, but for symptomatic cases, options include orthotics and surgical interventions. Myerson staging system is widely used to describe the progression of flatfoot. It divides AAFD into four stages (Table 2 [8]), although symptom severity does not always correlate with the extent of deformity, possibly because the patient soft tissues and bone structure have distorted to adapt to flatfoot deformity, or the cessation of inflammation in tendons.

Adult Acquired Flatfoot Deformity Staging and Treatment			
Stage	Deformity	Disease Progression	Treatment
I	None	Posterior tibialis tendon (PTT) tendinosis or tenosynovitis; Functional tendon	Conservative treatment initially Tenosynovectomy
II.			
IIA	Flexible moderate deformity (<40% of the talar head uncovered)	Tendinosis or a low-to-moderate-grade tear of the PTT; Laxity of the spring ligament	Orthoses Tendon transfer Medializing calcaneal osteotomy Subtalar arthroereisis Medial column stabilizing procedure
IIB	Flexible severe deformity (>40% of the talar head uncovered or subtalar impingement)	High-grade tear of PTT Incompetent spring ligament Sinus tarsi syndrome	Consider adding lateral column lengthening with or without spring ligament reconstruction
III	Rigid (inflexible) deformity	Subtalar osteoarthrosis Lateral hindfoot impingement	Subtalar arthrodesis or triple arthrodesis Consider adding medial ray procedure for plantar flexion of the first metatarsal
IV			
IVA	Flexible tibiotalar valgus	Deltoid ligament abnormality	Flatfoot reconstruction and deltoid ligament reconstruction
IVB	Rigid tibiotalar valgus	Tibiotalar osteoarthrosis	Consider adding tibiotalar fusion or ankle arthroplasty

Table 2: Adult Acquired Flatfoot Deformity Staging and Treatment (Simplified Blueman-Myerson Classification)

Section 3: Deformity Surgical Treatment for Flatfoot

Surgical procedures are suggested for symptomatic flatfoot deformity of stageII and above. Soft tissue and bony procedures are combined to correct flatfoot deformity based on each patient's stage and anatomic structures. The surgery is divided into two categories: osteotomy and arthroeresis. Osteotomy is a procedure where a bone is cut, reshaped, or removed to correct alignment, relieve pain, or address deformities. Arthroeresis is a surgical procedure that involves limiting or restricting the motion of a joint. In a typical foot arthroeresis (Figure 7), a small implant is placed into the sinus tarsi to block excessive pronation without completely immobilizing the joint. This procedure helps correct the foot's alignment and prevent pain or long-term issues associated with flatfoot deformity, which may be favored for pediatric flatfoot. For Stage IIIrigid flatfoot deformity, triple arthroeresis (Figure 8) fuses the subtalar, talonavicular, and calcaneocuboid articulations, which is used when the joints are severely degenerated. Triple arthroeresis can cause rigidity which can be complicated by malunion, nonunion, and talar dome necrosis [8]. Although arthroeresis implant avoids complications of triple arthroeresis, it has its own complications, which include persistent sinus tarsi pain, implant dislocation, implant fracture, talar cysts or osteonecrosis, and foreign body reaction [9]. Although in triple arthroeresis, fusion improves alignment of osseous structure, the loss of motion at fused joints will increase forces through remaining joints of the foot, and lead to degeneration at neighboring joints overtime [5].
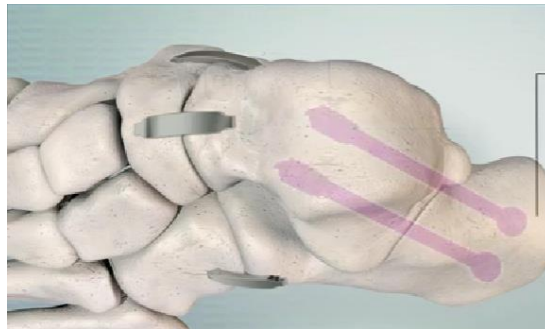
Figure 7. Arthroeresis Implant

Figure 8. Triple Arthroeresis

   To correct flexible flatfoot, a combination of soft tissue and bony procedures are adopted to reconstruct foot, correct deformities, and restore foot function, which may include steps: (1) gastrocnemius recession (gastrocnemius lengthening), (2) calcaneal lengthening (lateral column lengthening or Evan osteotomy), (3) medial cuneiform opening wedge osteotomy (Cotton osteotomy) and (4) posterior calcaneal osteotomy (posterior calcaneal realignment).
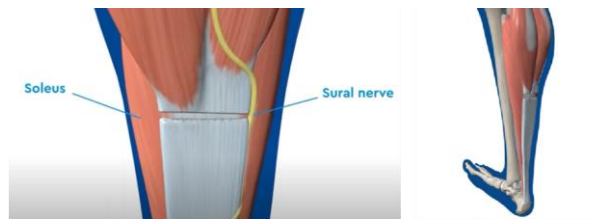
Step 1: Gastrocnemius Recession: The first step is the recession of the gastrocnemius muscle. An incision is made on the medial side of the leg, where the gastrocnemius muscle and the Achilles tendon converge. The gastrocnemius is carefully cut, ensuring that the underlying soleus muscle and the sural nerve laterally are protected. Then the ankle is dorsiflexed, and the foot is held in position, allowing the gastrocnemius to heal in a lengthened state on top of the soleus muscle.

Step 2: Evans Osteotomy: An incision is made on the lateral side of the calcaneus, with special attention given to avoid damage to the sural nerve and the peroneal tendons. The calcaneus bone is then cut. Trial wedges are inserted into the cut to adjust the forefoot abduction until talonavicular joint is closed as calcaneus is lengthened. A piece of bone graft of the proper size is wedged into the opening.

Step 3: Cotton Osteotomy: make a controlled cut in the medial cuneiform bone, and then inserting a wedge to elevate the first metatarsal, helping to restore the natural arch of the foot. Once the arch is restored properly, a proper sized bone graft replaces the wedge and insert into the cut.

Step 4: Posterior Calcaneal Osteotomy: If the calcaneus is still in an abnormal position after the previous steps, the posterior calcaneus is cut and is moved to central position and held in place with screws. The calcaneus then aligns with the axis of the lower leg.

Figure 9: Neuromuscular osteotomy

Extensive research has been performed to establish the protocol of osteotomy procedures to correct flatfoot.

Baxter et al. [10] explores the role of lateral column lengthening in treating AAFD. The study used cadaveric specimens to simulate flatfoot deformity by sectioning key ligaments and applied a lateral column lengthening osteotomy to assess its impact on both midfoot and hindfoot alignment.

Brilhault et al. [11] focus on in-depth analysis of various surgical approaches to correct hindfoot deformities, mainly focusing on calcaneal osteotomies. The medializing calcaneal osteotomy is often used to treat valgus flatfoot, realigning the calcaneus to the limb's mechanical axis and addressing the mechanical imbalances in the foot.

Guha et al. [12] focus on calcaneal osteotomies, particularly medial displacement calcaneal osteotomy (MDCO) and lateral column lengthening, as critical techniques for correcting these deformities. MDCO repositions the calcaneus to restore proper foot mechanics, transforming the gastrosoleus muscle from an evertor to an invertor of the heel, which is vital for correcting hindfoot valgus. The authors also suggest combining medical displacement calcaneal osteotomy with lateral column lengthening to improve flatfoot correction.

Tennant et al. [1] provide a detailed review of calcaneal osteotomy as a joint-preserving surgical technique used to correct deformities such as flatfoot. Techniques discussed include MDCO, lateral column lengthening (Evans osteotomy), closing wedge osteotomies (Dwyer), and complex osteotomy. Each technique realigns the calcaneus and improves foot biomechanics by restoring hindfoot stability and addressing medial arch collapse. The paper emphasizes careful preoperative planning and the importance of addressing soft tissue failures and heel cord tightness to achieve optimal outcomes and avoid complications.

B. Proposed Methods

Section 1: Pre-procedural Foot Model and Simulation

1. Deep Learning (AI) based flatfeet bone 3-dimensional (3D) modeling

When simulating the surgical correction of flat feet, the initial crucial step is to generate a 3D model of the foot bones. Surprisingly, the current literature offers very limited solutions for CT foot bone segmentation, and there are no publicly available datasets or open-source tools specifically for segmenting foot bones from CT scans. While Tiribilli et al. [4] proposed a workflow for foot bone segmentation and 3D modeling from orthopedic CT imaging, they did not provide open-source code or release a dataset. Drawing inspiration from their work, our goal is to develop a novel deep learning-based pipeline for foot bone segmentation and 3D reconstruction, leveraging a collected dataset of flatfoot CT images. Figure 10 depicts the deep learning-based 3D foot modeling reconstruction pipeline.
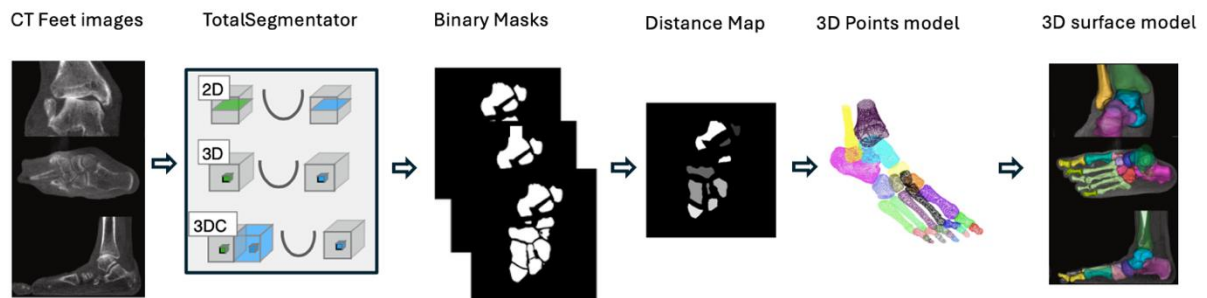

Figure 10. Pipeline of deep learning-based CT flatfeet segmentation and 3D modeling. Image source: CT Feet Images [11], TotalSegmentator [12], Binary masks [10], Distance Map [10], 3D surface model [11].

With given CT images of flatfeet, we utilized TotalSegmentator [13] to derive binary masks for the foot bones. TotalSegmentator effectively segments extremities and joints in high-resolution CT images, generating sub-compartment masks, including the part of ankle from the tibia bone, tarsal, metatarsal, and phalanges of the foot. To create a unified foot bone structure, we merged all generated masks into a single binary segmentation mask, applying morphological operations to remove small holes and noise. In a subsequent study, we developed an innovative method to convert these binary 3D foot CT bone segmentation masks into multi-labeled masks using advanced techniques, for example, distance map and watershed segmentation [14]. The process begins by taking binary mask as input (a Nifty file, where bone voxels are marked as one and the background as zero). We then

compute the Euclidean distance transform, assigning each voxel a value based on its distance from the nearest background voxel. Using the local maxima of the distance map as markers, we apply watershed segmentation to precisely separate individual bone structures, assigning a unique label to each bone. The resulting multi-labeled mask is saved as a Nifty file. This novel approach allows for precise isolation of individual bones from complex binary masks to enhance the accuracy of force analysis for flatfoot surgical simulations. Figure 11 is the Python code that demonstrating the conversion from a binary mask to a multi-label mask.

```python
import numpy as np
import nibabel as nib
import scipy.ndimage as ndi
from skimage.segmentation import watershed
from skimage.feature import peak_local_max


def binarymask_to_multi_labeled(input_nifti, output_nifti):
    """
    Load a NIfTI binary CT mask, generate a multi-labeled mask for individual bones using connected components and watershed,
    and save the result as a NIfTI file.

    Args:
    - input_nifti (str): Path to the input NIfTI file containing the binary CT mask.
    - output_nifti (str): Path to save the output NIfTI file containing the multi-labeled mask.
    """
    # Step 1: Load the binary 3D CT bone mask from a NIfTI file
    nifti_data = nib.load(input_nifti)
    binary_mask = nifti_data.get_fdata()
    affine = nifti_data.affine

    # Ensure binary mask is of type int (0 and 1)
    binary_mask = (binary_mask > 0).astype(np.int)

    # Step 2: Compute the distance transform of the binary mask
    distance_map = ndi.distance_transform_edt(binary_mask)

    # Step 3: Identify local maxima of the distance map for watershed segmentation
    local_maxi = peak_local_max(distance_map, indices=False, labels=binary_mask, footprint=np.ones((3, 3, 3)))

    # Step 4: Label the maxima for watershed markers
    markers, _ = ndi.label(local_maxi)

    # Step 5: Apply watershed segmentation to separate different bone structures
    multi_labeled_mask = watershed(-distance_map, markers, mask=binary_mask)

    # Step 6: Save the multi-labeled mask as a NIfTI file
    nifti_img = nib.Nifti1Image(multi_labeled_mask, affine)
    nib.save(nifti_img, output_nifti)
    print(f"Saved NIfTI file: {output_nifti}")


input_nifti_file = 'binary_feet_ct_mask.nii'
output_nifti_file = 'multi_labeled_bones_mask.nii'
binarymask_to_multi_labeled(input_nifti_file, output_nifti_file)
```

Figure 11. Python code to convert the flatfeet segmentation mask from binary to multi-label by using the distance map and watershed.

To reconstruct each 3D bone model from the resulting multi-label masks, our approach involves converting the individual masks into axial, sagittal, and coronal views. For each orientation, we extract binary masks and convert them into volumes of interest (VOI) contours. These VOI contours are then merged across the three views, creating a unified 3D cloud of points representing the shape of the bone. The point cloud generated from this process is subsequently fed into Ball-pivoting algorithm [15] and Screened Poisson surface reconstruction algorithm [16], which are particularly well-suited for handling sharp features and concave surfaces. The Poisson surface reconstruction algorithm has the advantage in generating smooth surfaces. The final output is a high-resolution 3D model for each bone, suitable for further visualization and analysis in the context of flatfoot modeling and surgical simulations.

Section 2: Dynamic 3D Simulated Surgical Environment

Flat foot correction involves multiple osteotomy procedures to restore proper foot alignment and function. We propose the development of a dynamic 3D simulation software that allows surgeons to trial different osteotomy procedures virtually, optimize wedge insertions, and adjust surgical strategies based on the patient's unique anatomy. The 3D dynamic simulation environment can give the real-time feedback to clinicians for informed decisions making for optimized correction. Integrating the simulation with Evans, Cotton, and Calcaneal procedures enables a more comprehensive approach to restoring foot biomechanics.

1. Evans Osteotomy

Evans Osteotomy is performed to correct forefoot abduction and lengthen the lateral column of the foot. An incision is made on the lateral side of the calcaneus, with careful attention to avoiding the sural nerve and peroneal tendons. The calcaneus bone is cut, and trial wedges of varying sizes (6 mm to 12 mm) are inserted into the cut to adjust forefoot abduction. The surgeon dynamically make adjustment until the talonavicular joint is closed, indicating the calcaneus has been lengthened sufficiently. Once the proper alignment is achieved, a bone graft of the appropriate size is wedged into the opening to secure the correction.

In the 3D simulation software, surgeons will be able to precisely model the calcaneal cut and key anatomical landmarks, including the lateral side of the calcaneus and the talonavicular joint. The software will allow virtual insertion of Evans wedges in different sizes, providing real-time feedback on the angles formed between the plane of the calcaneal cut and the surface of the inserted wedge. Figure 12 illustrated Evans wedges family ranging from 6 mm to 12 mm. By simulating different wedge sizes. Surgeons can adjust the graft position and wedge size, ensuring proper correction of the forefoot alignment and joint closure.
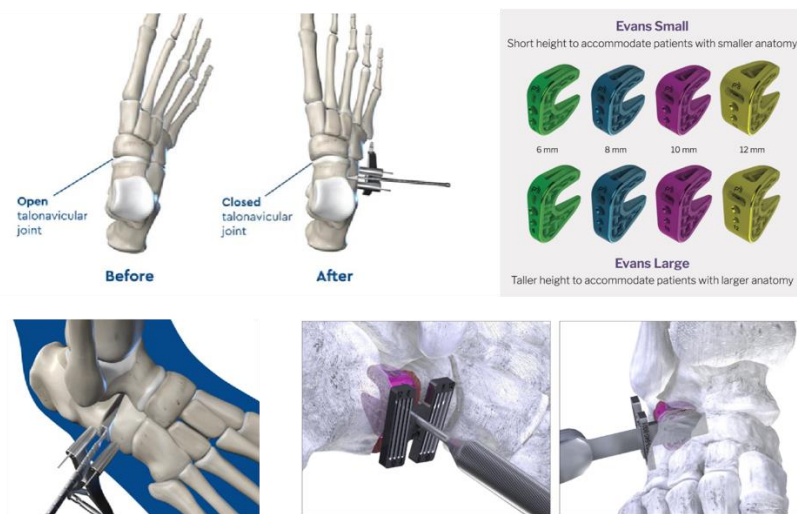

Figure 12. Simulated Evans wedge implant. The designed 3D simulation software will repeat the insertion and removing of Evans wedges of different size to optimize the best fit angle.

2. Cotton Osteotomy

Cotton Osteotomy is performed to correct the alignment of the medial column of the foot by restoring the natural arch. This procedure is conducted by making a controlled cut in the medial cuneiform bone, and inserting a wedge to elevate the first metatarsal, in order to re-establish the arch of the foot.

In the 3D simulation environment, surgeons can virtually trial different Cotton wedges, from 5 mm to 8 mm, as depicted in Figure 13. The software will allow the surgeon to adjust the insertion angle and the degree of elevation in real-time, providing immediate feedback on how each wedge size affects the medial column's alignment and the overall arch restoration to ensure that the arch is elevated correctly and corrected. Surgeons can make precise adjustments to the procedure and determine the optimal correction for the patient's foot anatomy by simulating different wedge sizes.
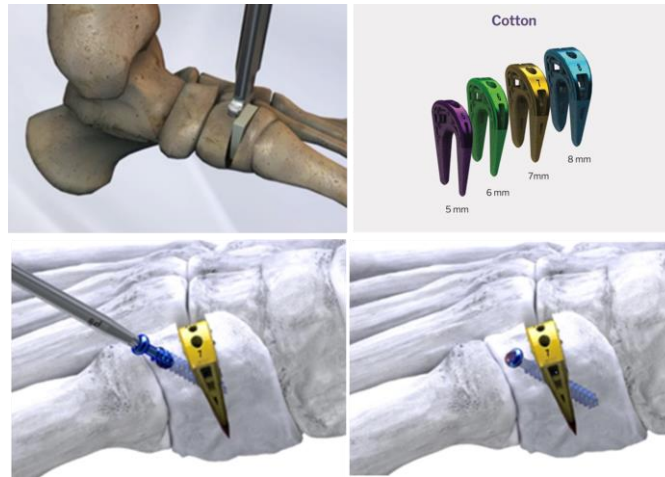
Figure 13. Simulated Cotton wedge implant. The designed 3D simulation software will trial the insertion and removing of Cotton wedges of different size to optimize the best fit angle.

3. Calcaneal Osteotomy

Calcaneal osteotomy is a procedure to correct heel deformities, for example, in flat feet or misaligned heel cases. During the operation, the surgeon cuts the posterior part of the calcaneus and shifts it either medially or laterally to align it with the lower leg axis properly. Once aligned, screws are inserted to stabilize the calcaneus, restoring the foot's natural structure and biomechanics.

Medializing calcaneal osteotomy (MCO) specifically corrects flatfoot deformities or other alignment issues by shifting the calcaneus medially. After the posterior calcaneus is cut, it is moved medially to restore the foot's proper alignment. A calcaneus step plate is used to stabilize the bone fragments post-osteotomy. This enables precise planning of the amount of medial translation needed to realign the calcaneus with the tibia and restore proper foot biomechanics.
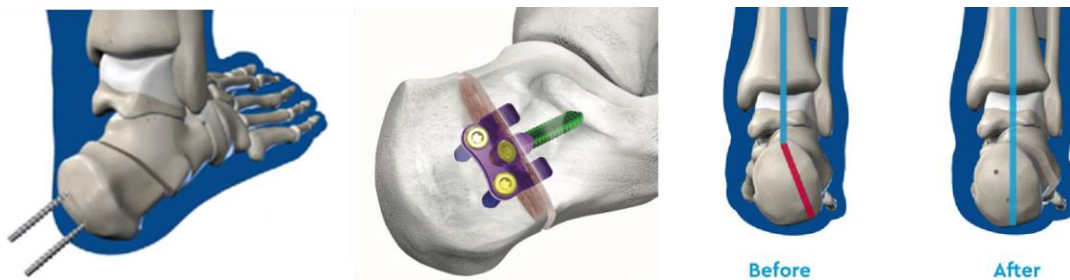

Figure 14. Simulated screw fixing and calcaneus step plate fixing the calcaneus

Section 3: Dynamic Simulation for Flat Feet Osteotomies

The proposed 3D dynamic simulation software combines the three osteotomy procedures—Evans, Cotton, and Calcaneal Osteotomies—allowing surgeons to virtually trial different wedge sizes, measure insertion angles, and receive real-time feedback on anatomical adjustments. The dynamic simulation facilitates a more precise and individualized surgical plan. The dynamic simulation is to restore the bony structure of foot to normal after reconstruction. Then, orthopedists can follow the simulation to perform osteotomies, improving the precision of the procedure.

C. Intra-procedural Stress Concentration and Load distribution Detection

As elaborated previously, it is not feasible to do a full body weight bear test during the osteotomy operation. However, according to the different biomechanics of normal foot and flat foot, the stress concentration and load

distribution are on different regions of the normal foot and flat foot. In normal foot, the stress is concentrated at the heel, ball of foot and toes. The load is distributed evenly at longitude of the foot and across the width of the foot along the lateral longitudinal arch and transvers arch. In flatfoot, the load distribution shifts to medial side of foot, and stresses especially concentrate at the medial side of the calcaneus, medial longitudinal arch, navicular bone, and the first metatarsal.

If measured quantitively, the ratios of the stress concentration in different foot regions are distinctive between normal foot and flat foot. So, the solution to measure intra-procedural stress concentration of reconstructed foot to see whether it is structurally restored to normal can convert to a comparison between the ratio of stress concentration of reconstructed foot and the original flat foot. Orthopedics can replace the flat metal plate with force plates to measure the stress at different foot regions by giving a bearable force to intra-procedural foot. The orthopedics can compute the ratio of stress concentration to compare with the ratio of the original flat feet. The ultimate goal is to adjust the ratio of press concentration in different regions of the reconstructed foot to normal range.

Through literature review, the ranges of ratios of stress concentration in different regions of foot overlapped for normal foot and flatfoot. The statistics are not granular enough to be used to judge whether the reconstructed foot is adjusted well. If using the foot plantar pressure information to calculate the ratio, the most challenge is that probably no one measures normal foot plantar pressure in the same intra-surgical environment, i.e. people lying down with foot 90 degrees and apply the same intense forces as to measure the intra-surgical corrected flatfoot. The foot plantar pressures vary significantly under different force or load.
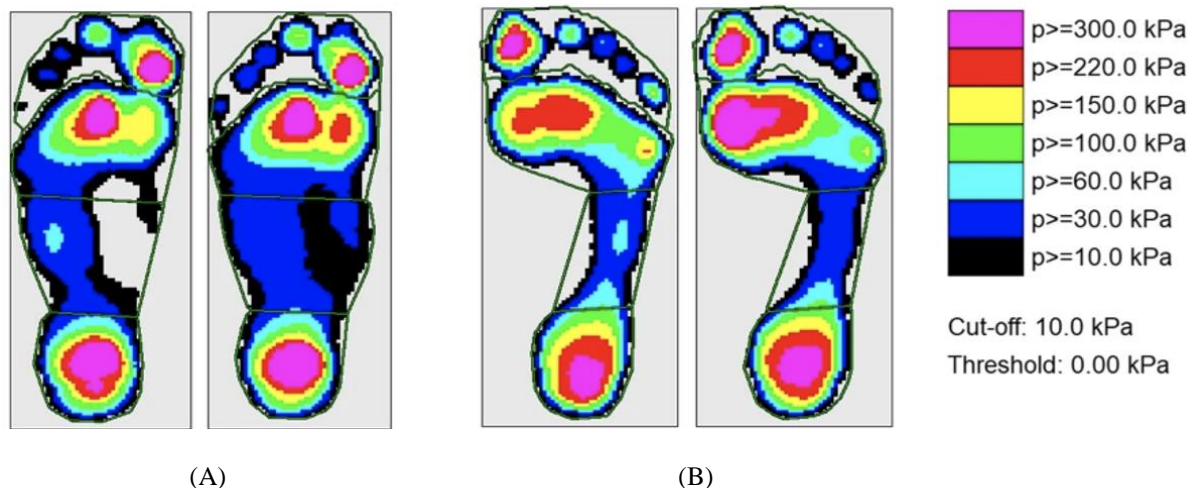

(A)   (B)

Figure 15. Foot Plantar Pressure
A. Flat foot no load (left) 20kg backpack load (right)
B. Normal foot no load (left) 20kg backpack load (right)

Therefore, we suggest research to collect large data of plantar pressure in normal foot and flatfoot in same intra-surgical environment. The heights, weights, body shapes, foot size and athletic records should be collected simultaneously because these metrics may affect the ratios of stress concentration in foot and AI can match the patient bio data with people of similar bio traits and good athletic performance.

In the future, if a pre-procedure foot 3D model and simulation can incorporate the prediction of the targeted ratios of the press concentration in foot, A personalized operation plan can be designed accordingly.

D. Intra-procedural synthetic AI model to assist the flatfeet restoration

In developing a synthetic AI model to predict the target normal foot structure from flatfoot conditions, we integrate key parameters from the Evans, Cotton, and Calcaneal osteotomies along with plantar pressure distribution data. The parameters for each osteotomy procedure—such as pre- and post-surgical foot alignment, angles, lengths, and biomechanics—are captured in Table 3 to 6. Parameters marked with N/A in the source column do not have a pre-surgery measurement because they represent outcomes that are only applicable after surgery. Additionally, the pressure distribution data, collected preoperatively and postoperatively as outlined in

Tables 7, offers critical insights into load-bearing patterns and plantar pressure ratios.   Table 8 depicts a simple synthetic quantitative data for Evans Osteotomy parameters.

The input parameters (source) of the AI model include key osteotomy measurements and pressure distribution data from flatfoot patients, such as forefoot abduction angle, medial arch height, calcaneal alignment, and various pressure metrics, that represent foot's structure and biomechanical state before surgery. The output parameters (target) consist of the desired post-surgical attributes for these same measurements that represent a normal foot's structure and pressure distribution, including corrected angles, arch height, heel alignment, and normalized pressure ratios. These inputs and outputs demonstrate a comprehensive view for predicting surgical outcomes.

Those osteotomy parameters and pressure distribution data lay out the synthetic foundation to model the surgical interventions that could affect the foot alignment and pressure distribution.   The general AI model can use synthetic data to train and predict each patient's optimal post-surgery foot structure. Tables 3 to 8 demonstrate the modeling of the synthetic data, which constitutes the foundation for data collection,

Procedure	Parameter	Description
Evans Osteotomy	Initial Forefoot Abduction Angle	Degree of abduction of the forefoot before surgery
	Calcaneal Lengthening Amount (Wedge Size)	Size of the wedge inserted (6 mm to 12 mm)
	Talonavicular Joint Alignment	Degree of closure at the talonavicular joint
	Calcaneal Cut Angle	Angle of the bone cut relative to the plane of the calcaneus
	Foot Orientation Before and After Surgery	3D positioning of the foot before and after surgery
	Wedge Positioning	Final placement and positioning of the wedge
	Postoperative Forefoot Alignment	Corrected abduction angle after surgery
Cotton Osteotomy	Preoperative Medial Arch Height	Initial height of the medial arch before surgery
	First Metatarsal Elevation Angle	Degree of elevation of the first metatarsal
	Cuneiform Cut Angle	Angle at which the medial cuneiform is cut
	Wedge Size (Elevation Amount)	Size of the wedge used to elevate the medial column
	Postoperative Medial Arch Height	Final arch height after osteotomy and grafting
	Foot Orientation Before and After Surgery	3D foot orientation before and after surgery
	Talonavicular Joint Positioning	Alignment of the talonavicular joint post-surgery
Calcaneal Osteotomy	Initial Calcaneal Alignment (Heel Position)	Position of the calcaneus relative to the tibia and fibula before surgery
	Osteotomy Cut Angle	Angle of the cut on the calcaneus bone
	Medial or Lateral Shift Amount	Distance the calcaneus is shifted medially or laterally
	Foot Orientation Before and After Surgery	3D foot alignment relative to the leg axis
	Screw and Plate Placement	Positioning of screws and plates for fixation
	Postoperative Heel Alignment	Final heel position and alignment with the tibial axis
	Foot Orientation Before and After Surgery (General)	General 3D foot alignment for all procedures

Table 3. Osteotomy Parameters Explanation for AI Model

Evans Osteotomy

Parameter	Source (Pre-Surgery Flatfoot)	Target (Post-Surgery Normal Foot)
Forefoot Abduction Angle	Initial Forefoot Abduction Angle	Target Forefoot Abduction Angle
Calcaneal Lengthening (Wedge Size)	Calcaneal Lengthening Amount	Target Calcaneal Lengthening Amount
Talonavicular Joint Alignment	Talonavicular Joint Alignment	Target Talonavicular Joint Alignment
Calcaneal Cut Angle	Calcaneal Cut Angle	Target Calcaneal Cut Angle
Foot Orientation (3D Positioning)	Foot Orientation Before Surgery	Target Foot Orientation After Surgery
Wedge Positioning	Wedge Positioning	Target Wedge Positioning
Postoperative Forefoot Alignment	N/A	Target Postoperative Forefoot Alignment

Table 4. Evans Osteotomy Parameters (Source-input, Target-output)

Cotton Osteotomy

Parameter	Source (Pre-Surgery Flatfoot)	Target (Post-Surgery Normal Foot)
Medial Arch Height	Preoperative Medial Arch Height	Target Medial Arch Height
First Metatarsal Elevation Angle	First Metatarsal Elevation Angle	Target First Metatarsal Elevation Angle
Cuneiform Cut Angle	Cuneiform Cut Angle	Target Cuneiform Cut Angle
Wedge Size (Elevation Amount)	Wedge Size (Elevation Amount)	Target Wedge Size for Normal Foot
Foot Orientation (3D Positioning)	Foot Orientation Before Surgery	Target Foot Orientation After Surgery
Talonavicular Joint Positioning	Talonavicular Joint Positioning	Target Talonavicular Joint Positioning
Postoperative Medial Arch Height	N/A	Target Postoperative Medial Arch Height

Table 5. Cotton Osteotomy Parameters (Source-input, Target-output).

Calcaneal Osteotomy

Parameter	Source (Pre-Surgery Flatfoot)	Target (Post-Surgery Normal Foot)
Calcaneal Alignment (Heel Position)	Initial Calcaneal Alignment	Target Calcaneal Alignment
Osteotomy Cut Angle	Osteotomy Cut Angle	Target Osteotomy Cut Angle
Medial or Lateral Shift Amount	Medial or Lateral Shift Amount	Target Medial or Lateral Shift Amount
Foot Orientation (3D Alignment)	Foot Orientation Before Surgery	Target Foot Alignment After Surgery
Screw and Plate Placement	Screw and Plate Placement	Target Screw and Plate Placement
Heel Alignment	N/A	Target Heel Alignment

Table 6. Calcaneal Osteotomy Parameters (Source-input, Target-output)

Pressure Parameters

Parameter	Source (Pre-Surgery Flatfoot)	Target (Post-Surgery Normal Foot)
Heel Pressure	Heel Pressure	Target Heel Pressure
Midfoot Pressure (Medial)	Midfoot Pressure (Medial)	Target Midfoot Pressure (Medial)
Midfoot Pressure (Lateral)	Midfoot Pressure (Lateral)	Target Midfoot Pressure (Lateral)
Midfoot Pressure (Central)	Midfoot Pressure (Central)	Target Midfoot Pressure (Central)
Forefoot Pressure (1st Metatarsal)	Forefoot Pressure (1st Metatarsal)	Target Forefoot Pressure (1st Metatarsal)
Forefoot Pressure (2nd Metatarsal)	Forefoot Pressure (2nd Metatarsal)	Target Forefoot Pressure (2nd Metatarsal)
Forefoot Pressure (3rd Metatarsal)	Forefoot Pressure (3rd Metatarsal)	Target Forefoot Pressure (3rd Metatarsal)
Forefoot Pressure (4th Metatarsal)	Forefoot Pressure (4th Metatarsal)	Target Forefoot Pressure (4th Metatarsal)
Forefoot Pressure (5th Metatarsal)	Forefoot Pressure (5th Metatarsal)	Target Forefoot Pressure (5th Metatarsal)
Toes Pressure	Toes Pressure	Target Toes Pressure
Heel-to-Forefoot Pressure Ratio	Heel-to-Forefoot Pressure Ratio	Target Heel-to-Forefoot Pressure Ratio
Medial-to-Lateral Midfoot Pressure Ratio	Medial-to-Lateral Midfoot Pressure Ratio	Target Medial-to-Lateral Midfoot Pressure Ratio
Medial-to-Lateral Forefoot Pressure Ratio	Medial-to-Lateral Forefoot Pressure Ratio	Target Medial-to-Lateral Forefoot Pressure Ratio
First to Fifth Metatarsal Pressure Ratio	First to Fifth Metatarsal Pressure Ratio	Target First to Fifth Metatarsal Pressure Ratio
Center of Pressure (CoP) Path	CoP Path and Trajectory	Expected CoP Path and Trajectory
Initial CoP Location	Initial CoP Location	Expected Initial CoP Location
Total Contact Area	Total Contact Area	Target Total Contact Area
Medial vs Lateral Contact Area	Medial vs Lateral Contact Area	Expected Medial vs Lateral Contact Area
Midfoot Contact Area	Midfoot Contact Area	Expected Midfoot Contact Area
Maximum Pressure in Regions	Maximum Pressure in Regions	Expected Maximum Pressure in Regions
Mean Pressure in Regions	Mean Pressure in Regions	Expected Mean Pressure in Regions
Pressure Gradient from Heel to Toes	Pressure Gradient from Heel to Toes	Target Pressure Gradient from Heel to Toes
Medial-to-Lateral Pressure Gradient	Medial-to-Lateral Pressure Gradient	Target Medial-to-Lateral Pressure Gradient
Foot Length	Foot Length	Expected Foot Length
Foot Width	Foot Width	Expected Foot Width
Arch Height	Arch Height	Expected Arch Height
Weight Distribution	Weight Distribution	Expected Weight Distribution

Table 7. Pressure Parameters (Source-input, Target-output)

Example with Units and Descriptions:

Evans Osteotomy Parameters

Parameter	Source (Flatfoot)	Target (Normal Foot)	Unit	Description
Forefoot Abduction Angle	Initial Angle (e.g., 15°)	Target Angle (e.g., 5°)	Degrees	Degree of forefoot abduction
Calcaneal Lengthening Amount	Wedge Size (e.g., 8 mm)	Target Wedge Size (e.g., 6 mm)	Millimeters	Amount of lengthening via wedge insertion
Talonavicular Joint Alignment	Alignment Angle (e.g., 25°)	Target Alignment Angle (e.g., 5°)	Degrees	Alignment of the talonavicular joint
Calcaneal Cut Angle	Cut Angle (e.g., 30°)	Target Cut Angle (e.g., 10°)	Degrees	Angle of calcaneal bone cut
Foot Orientation (3D Position)	Pre-Surgery Orientation (x, y, z coordinates)	Post-Surgery Orientation (x, y, z coordinates)	N/A	3D positioning of the foot
Wedge Positioning	Position (e.g., posterior)	Target Position (e.g., anterior)	N/A	Placement of the wedge
Postoperative Forefoot Alignment	N/A	Alignment Post-Surgery (e.g., neutral alignment)	N/A	Alignment after surgery

Table 8. Pressure Parameters (Source-input, Target-output)

To develop an effective AI model, we need a robust dataset containing pressure measurements for both normal and flatfoot individuals in similar environments (e.g., lying down with the foot at 90°) to simulate intra-procedural conditions. By matching patient profiles (height, weight, foot size), the AI can learn to predict the most optimal load distribution and pressure ratios for reconstructed feet, using data from individuals with similar biomechanical profiles.

To train the AI model, we convert the osteotomy features and pressure measurement parameters into attribute-value pairs for each patient. These pairs are organized into two distinct paragraphs: one representing the pre-surgery flatfoot conditions (input) and the other capturing the post-surgery target outcomes (output). The relevant attribute-value pairs constitute each paragraph that is suited for the natural language processing. We leverage the Large Language Models (LLMs) general capability to analyze and build the complicated relationships between the data points from input and output attributes. The model can learn from the surgical intervention parameters that impact the foot structure and pressure distribution. Overall, this AI driven modeling during intraoperative operation could enable or enhance the more approximate predictions of post-surgical outcomes.

With approximately 10,000 patients' data, constitutes both pre- and post-surgery measurements, we can create a synthetic (reasonable) training dataset. By encoding the relevant osteotomy parameters (e.g., forefoot abduction angle, medial arch height, calcaneal alignment) and pressure metrics (e.g., heel-to-forefoot pressure ratios, center of pressure path) as natural language inputs, the model can learn how surgical interventions impact foot structure and pressure distribution.

At the current stage, we are focusing on utilizing the LLaMA Large Language Model (LLM) to train the AI model. By framing each patient's data as a single coherent paragraph, the LLM can be trained to predict optimal post-surgical outcomes based on the structured, language-like representation of each patient's flatfoot condition and surgical results. Figure 16 illustrates a synthetic LLaMA 3 based training workflow and LLaMA 3 architecture [17].

The choice of LLaMA 3 as our foundational AI model is motivated by its efficiency and open-source nature, which provides full access to the model for training and fine-tuning on flatfoot surgery data. This open framework also allows flexibility in replacing the foundational model with other LLMs in the future as needed. For instance, OpenAI's GPT-4 [18] is one alternative that enables fine-tuning via the OpenAI API, however, it does not warrant access to raw model weights when training from scratch. Google's T5 (Text-to-Text Transfer Transformer) [19]

is another flexible option, treating all NLP tasks as text-to-text problems and offering fine-tuning capabilities. Other models, such as Anthropic's Claude [20] and BERT [21] (along with its derivatives), are also viable as foundational AI models for this project. This alternative AI approach preserves the flexibility to explore and switch between different LLMs as foundational models, allowing for future adaptation to advancements in AI technology.
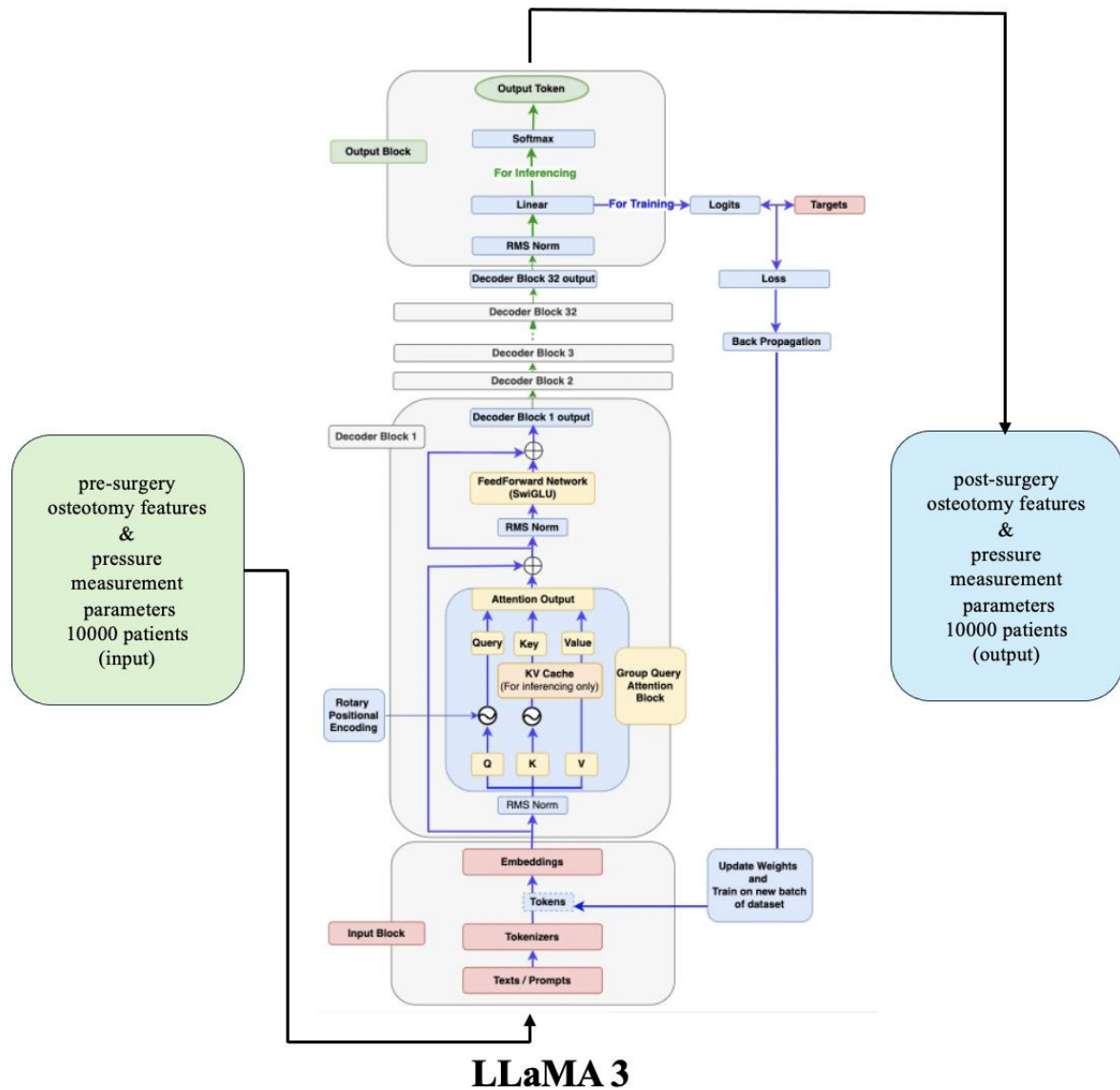

Figure 16. LLaMA3 training workflow and LLaMA3 architecture.

By combining these osteotomy-specific features with pressure distribution data, the AI model is able to learn how surgical interventions affect foot biomechanics and load distribution between flatfoot and normal foot. This combined synthetic dataset allows the AI to learn from both structural changes imposed by the surgeries and biomechanical feedback, landing a comprehensive basis for predicting the optimal post-surgical foot structure. This synthetic or feasibly sound AI training framework provides the relationship between the patient's pre-surgical flatfoot condition and the desired post-surgical outcomes, helping the AI model to personalize the best surgical approach for each patient.

III. CONCLUSION

This study tackles two fundamental challenges in flatfoot osteotomies: leveraging artificial intelligence (AI) to design preoperative models of the foot's restored bony structure and quantitatively measuring stress concentration and load distribution on the plantar surface during surgery. AI-driven 3D modeling and simulation help achieve optimal alignment based on each patient's anatomy. Furthermore, intraoperative evaluation of stress distribution leaves real-time insights into whether the bony corrections will support normal foot function, reducing variability in post-surgical outcomes. In this work, we explore the potential to integrate the AI-driven model for intra-procedural flatfoot osteotomy surgery. We'd rather lay out the foundation framework in general. The osteotomy parameters and pressure distribution data collection still need further investigation, for example, how to measure and collect those parameters during surgery. We wish the proposed AI and data driven method can depict a strategic path for flatfoot orthopedic surgery, paving the way for more personalized, efficient, and biomechanically optimized flatfoot correction.

However, to restore the osseous structure of foot does not equal to restore the function of the foot. The effects of foot osteotomy on biomechanical stress patterns in bones and soft tissues have been less thoroughly studied. Bayod et al. [22] use a finite element model to evaluate stress redistribution in the foot after MCO. The findings show that MCO effectively reduces hindfoot valgus and forefoot pronation, while simultaneously creating a supination moment that stabilizes the foot structure. The study also highlights that when the plantar fascia or posterior tibial tendon fail, stress significantly increases in the lateral metatarsals and around the osteotomy site, which could lead to long-term complications such as pain or fractures. The proposed AI driven model lacks the consideration of soft tissue failure when planning surgical interventions like MCO, as they can alter stress distributions and affect outcomes. Further studies in soft tissue recovery are necessary.

REFERENCES

1. Tennant, J.N., M. Carmont, and P. Phisitkul, *Calcaneus osteotomy.* Curr Rev Musculoskelet Med, 2014. **7**(4): p. 271-6.
2. Romeo, G., et al., *Medial Cuneiform Opening Wedge Osteotomy for Correction of Flexible Flatfoot Deformity: Trabecular Titanium vs. Bone Allograft Wedges.* Biomed Res Int, 2019. **2019**: p. 1472471.
3. Xu, C., et al., *Biomechanical effects of Evans versus Hintermann osteotomy for treating adult acquired flatfoot deformity: a patient-specific finite element investigation.* Journal of Orthopaedic Surgery and Research, 2024. **19**(1).
4. Tiribilli, E. and L. Bocchi, *Deep Learning-Based Workflow for Bone Segmentation and 3D Modeling in Cone-Beam CT Orthopedic Imaging.* Applied Sciences, 2024. **14**(17).
5. Ker, R.F., et al., *The spring in the arch of the human foot.* Nature, 1987. **325**(6100): p. 147-149.
6. AJ, M., *Knock-knee in children.* Br Med J, 1957. **2**: p. 976–979.
7. Hosalkar HS, S.D., Davidson R, *The foot and toe. Nelson textbook of pediatrics*, ed. S.B. Kliegman RM, Schor NF, et al. 2011, Philadelphia, USA: Elsevier Saunders.
8. Flores, D.V., et al., *Adult Acquired Flatfoot Deformity: Anatomy, Biomechanics, Staging, and Imaging Findings.* Radiographics, 2019. **39**(5): p. 1437-1460.
9. Vulcano, E., J.T. Deland, and S.J. Ellis, *Approach and treatment of the adult acquired flatfoot deformity.* Curr Rev Musculoskelet Med, 2013. **6**(4): p. 294-303.
10. Baxter, J.R., et al., *Lateral column lengthening corrects hindfoot valgus in a cadaveric flatfoot model.* Foot Ankle Int, 2015. **36**(6): p. 705-9.
11. Brilhault, J., *Calcaneal osteotomy for hindfoot deformity.* Orthop Traumatol Surg Res, 2022. **108**(1S): p. 103121.
12. Guha, A.R. and A.M. Perera, *Calcaneal osteotomy in the treatment of adult acquired flatfoot deformity.* Foot Ankle Clin, 2012. **17**(2): p. 247-58.
13. Wasserthal, J., et al., *TotalSegmentator: Robust Segmentation of 104 Anatomic Structures in CT Images.* Radiol Artif Intell, 2023. **5**(5): p. e230024.
14. Kornilov, A., I. Safonov, and I. Yakimchuk, *A Review of Watershed Implementations for Segmentation of Volumetric Images.* J Imaging, 2022. **8**(5).

15. Digne, J., *An Analysis and Implementation of a Parallel Ball Pivoting Algorithm.* Image Processing On Line, 2014. **4**: p. 149-168.
16. Xu, Z., C. Xu, J. Hu, and Z. Meng, *Robust resistance to noise and outliers: Screened Poisson Surface Reconstruction using adaptive kernel density estimation.* Computers & Graphics, 2021. **97**: p. 19-27.
17. Dubey, A., et al., *The Llama 3 Herd of Models*. in *ArXiv abs/2407.21783 (2024): n. pag.*
18. Achiam OpenAI, Josh, et al., *GPT-4 Technical Report*. 2023.
19. Itsnaini, Q., et al., *Abstractive Text Summarization using Pre-Trained Language Model "Text-to-Text Transfer Transformer (T5)".* ILKOM Jurnal Ilmiah, 2023.
20. Priyanshu, A., et al., *AI Governance and Accountability: An Analysis of Anthropic's Claude*. in *ArXiv abs/2407.01557: n. pag.* 2024.
21. Devlin, J., et al., *BERT: Pre-training of Deep Bidirectional Transformers for Language Understanding*. in *North American Chapter of the Association for Computational Linguistics* 2019.
22. Bayod, J., R. Larrainzar-Garijo, B.D. Solórzano, and C. Cifuentes-De la Portilla, Biomechanical Effects of Medializing Calcaneal Osteotomy on Bones and the Tissues Related to Adult-Acquired Flatfoot Deformity: A Computational Study. Mathematics, 2023. 11(10).

SOURCES OF FIGURES

1. Figure 2: https://redmountainfootcare.com/flat-feet/flat-feet-symptoms-treatments-more

2. Figure 3: Adult Acquired Flatfoot Deformity: Anatomy, Biomechanics, Staging, and Imaging Findings. Radiographics, 2019. 39(5): p. 1437-1460

3. Figure 4: https://www.youtube.com/watch?v=HXlKVVoVnpU

4. Figure 5 & 6: Adult Acquired Flatfoot Deformity: Anatomy, Biomechanics, Staging, and Imaging Findings. Radiographics, 2019. 39(5): p. 1437-1460

5. Figure 7: https://www.youtube.com/watch?v=c_FnMXRMT7I

6. Figure 8: https://www.youtube.com/watch?v=ko2PNLr7Oaw

7. Figure 9. Neuromuscular Osteotomy to Correct Flatfoot: https://www.youtube.com/watch?v=TWUE-z3aMe8

    https://www.broadcastmed.com/orthopedics/8064/videos/allopure-allograft-bone-wedges-animation-specific-for-evans-and-cotton-osteotomies-009117

8. Figure 12: https://paragon28.com/app/uploads/2021/08/P28FL-02-Rev-B_FlatfootBrochure.pdf
    https://www.youtube.com/watch?v=TWUE-z3aMe8

9. Figure 13: https://www.broadcastmed.com/orthopedics/8064/videos/allopure-allograft-bone-wedges-animation-specific-for-evans-and-cotton-osteotomies-009117

    https://paragon28.com/app/uploads/2021/08/P28FL-02-Rev-B_FlatfootBrochure.pdf

10. Figure 14: https://www.youtube.com/watch?v=TWUE-z3aMe8

    https://paragon28.com/app/uploads/2021/08/P51-STG-0004-RevE_Gorilla-Calc-Slide-Plate-STG-US.pdf

11. Figure 15. The effect of backpack load on intersegmental motions of the foot and plantar pressure in individuals with mild flatfoot. https://jfootankleres.biomedcentral.com/articles/10.1186/s13047-022-00579-8